BELLCOMM, INC.
955 L'ENFANT PLAZA NORTH, S.W. WASHINGTON, D.C. 20024

SUBJECT: Disposal of Spent S-IVB Stage on Lunar Missions - Case 310

DATE: December 11, 1968

FROM: L. P. Gieseler

## ABSTRACT

The spent S-IVB stage is nominally on a free-return trajectory after spacecraft separation. Previous studies have shown that with guidance dispersions there is a 38 percent probability of lunar impact and a 30 percent probability of earth impact.

Dumping S-IVB cold residual propellants through the engine after separation provides a means of obtaining a velocity correction to the S-IVB trajectory which may be used to avoid both earth and lunar impact and still assure that spacecraft recontact will not occur. Safe disposal of the S-IVB may be achieved by establishing a trajectory in which enough energy is gained by the S-IVB from a lunar encounter to cause its escape from the earth-moon system. This has been termed a "slingshot trajectory".

This paper is concerned with the determination of the magnitude and direction of the velocity correction necessary to assure safe disposal of the S-IVB using a "slingshot trajectory". Variations in the required velocity correction caused by launch date are studied in terms of the translunar dihedral angle, which is the angle between the translunar and lunar orbital planes.

Two implementations are discussed: (1) A controlled termination of the propellant dump which allows using a maneuver $\Delta V$ at a fixed attitude in all cases, and (2) An uncontrolled dump with the maneuver $\Delta V$ direction being a computed function of the dihedral angle, the time of the maneuver, and the expected total $\Delta V$.

It is concluded that the controlled dump will be necessary to assure a slingshot because of the likelihood of large S-IVB residual propellants. It is also concluded that launch vehicle and spacecraft recontact is avoided when the maneuver is applied to obtain a slingshot trajectory.

BELLCOMM, INC.
955 L'ENFANT PLAZA NORTH, S.W. WASHINGTON, D. C. 20024

SUBJECT: Disposal of Spent S-IVB Stage on Lunar Missions - Case 310

DATE: December 11, 1968

FROM: L. P. Gieseler

MEMORANDUM FOR FILE

## I. INTRODUCTION

An Apollo lunar mission requires that after translunar injection (TLI) the vehicle undergo a transposition, docking, and withdrawal maneuver. The vehicle separates into two parts, the CSM/LM combination which proceeds to the moon, and the spent S-IVB booster which in the absence of any propulsion after withdrawal would nominally follow a free-return trajectory, entering the earth's atmosphere with a shallow flight path angle. However, according to Reference (1), the guidance dispersions at TLI are large enough so that there is a 38% probability of a lunar impact and a 30% probability of an earth impact.

The Apollo Flight Mission Assignments document (Reference 2) states the requirement for S-IVB disposal in terms of three objectives. These objectives stated in decreasing order of priority are: (1) Avoid S-IVB/spacecraft recontact, (2) Avoid earth impact, and (3) Avoid lunar impact. In order to achieve the three objectives, various modifications to the S-IVB orbit after separation can be considered. The most promising would be the establishment of a trajectory which escapes the earth-moon system entirely. This method employs an encounter with the moon to raise the S-IVB energy to the level required for escape. Trajectories of this type have been termed "slingshot trajectories" (Reference 3).

In previous studies (References 1 and 4) integrated trajectories were calculated in which the dihedral angle, $DL_1$, between the spacecraft orbit and the lunar orbit was a dependent variable and therefore not directly controllable. For this study $DL_1$ was treated as an independent variable. Values of 0, 30, 45, and 60 degrees were used, and the results may be considered representative of trajectories which are launched with all practical launch dates and launch azimuths. An average earth-moon distance was used.

The S-IVB propellants remaining after launch vehicle/spacecraft separation may be dumped through the engine of the S-IVB to produce a thrust. It is by this means that the velocity

correction required to satisfy the objectives for S-IVB disposal is obtained.

Theoretically the orbit of the S-IVB could be determined after separation by MSFN tracking data and ground computations and a corrective impulse applied so that the three objectives are fully satisfied. Another approach which is equivalent if errors at TLI are not considered would be to precompute for the nominal trajectory the corrective impulse required to achieve the objectives, and program the onboard logic accordingly. This would require the preprogrammed termination of propellant dumping by a command based on measured $\Delta V$. (Alternately the dump can be terminated at a preprogrammed time, but any errors in the assumed thrust profile of the dump will be reflected directly in errors in the impulse applied.)

A third approach, which would result in considerably simpler implementation but a greater uncertainty of accomplishing all of the objectives, would reorient the vehicle to a preplanned attitude and begin the dumping at a predetermined time. The dumping would be continued until all propellants are exhausted. (Either LOX or $LH_2$ or both may be dumped) In this case variations in the propellants remaining in the S-IVB could result in a large variation in the $\Delta V$ produced.

The S-IVB Auxiliary Propulsion system (APS) is still operable after separation and can be used to orient the vehicle in a preferred direction. The APS is also available for producing additional translational thrust.

In this paper the first two approaches are equivalent since no consideration of guidance errors is made. The resulting families of trajectories for a monitored and terminated propellant dump and for a non-terminated dump are determined. Once a means of establishing a suitable trajectory has been demonstrated it is shown that recontact between the spacecraft and S-IVB can be avoided.

## II. CALCULATION OF VELOCITY INCREMENT

The relation between $\Delta V$ and the amount of propellant remaining after TLI is given by the rocket equation:

$$\Delta V = gI_{sp} \log_e \frac{m_1}{m_2}$$

$$= gI_{sp} \log_e \left(1 + \frac{\Delta m}{m_2}\right) \qquad (1)$$

where $m_1$, $m_2$ are the masses of the S-IVB before and after the

impulse, g = 32.2 fps, $I_{sp}$ = specific impulse of the S-IVB when dumping propellant in an unburned condition, and $\Delta m = m_1 - m_2$ = mass of propellant discharged through the nozzle.

Equation (1) was used to compute the $\Delta V$ for representative values of the propellants corresponding to the trapped residuals, the unused flight performance reserves, the unused flight geometry reserves, and the propellant remaining due to launch azimuth variation. The results are given in Table I. The weights shown are estimates based on October 1968 weight and performance data (Reference 7). The "Excess Performance" results from the predicted differential between Saturn V performance capability and the structural limitation of 102,000 lbs. Additional propellants shown in the Table are included because current weight estimates indicate that the spacecraft fully fueled could be as much as 1000 lbs. less than the 102,000 lbs. hypothesized.

Based on the tabulated data, the minimum $\Delta V$ available is 143 fps. The maximum for dumping $LH_2$ alone, LOX alone, and both LOX and $LH_2$ is 120, 215, and 335 fps, respectively. The Auxiliary Propulsion System (APS) is also available and can, if needed, supply translational $\Delta V$.

## III. GENERATION OF SLINGSHOT TRAJECTORIES

### a. Geometrical Concepts

The patched-conic approximation is a useful device for studying earth-moon trajectories. Figure 1a illustrates the free-return case. For simplicity only the portion of the orbit in and near the moon's sphere of influence (MSI) is shown. It is also assumed in the figure that the orbital planes of the vehicle and the moon coincide. Deviations from this condition will be considered later. $\overline{V}_{e1}$ is the vector velocity on the translunar ellipse at the MSI entry point $P_1$. $V_{m1}$, the corresponding vector velocity on the hyperbolic orbit inside the MSI, is obtained by the formula

$$\overline{V}_{m1} = \overline{V}_{e1} - \overline{V}_L \qquad (2)$$

where $\overline{V}_L$ is the velocity of the moon.

Figure 1a shows a symmetrical free-return trajectory, in which the periselene of the hyperbola lies on the earth-moon line. $\overline{V}_{e2}$ and $\overline{V}_{m2}$ are corresponding velocities at the MSI exit point $P_2$, and are related by the equation

$$\overline{V}_{e2} = \overline{V}_{m2} + \overline{V}_L \qquad (3)$$

Figure 1b shows the orbit that is produced when a velocity impulse of 50 feet per second is applied to the vehicle in a direction opposite to the velocity vector two hours after TLI. The vehicle now travels somewhat more slowly with the result that it reaches the MSI about 1-1/2 hours later. During this time the moon has moved to the position shown, referenced to location M of Figure 1a. It can be seen that $V_{m1}$ is now directed to the right of $R_1$, the selenographic radius vector, and the vehicle consequently travels around the moon in a counter-clockwise direction. The magnitude of $\overline{V}_{m2}$ is the same as $\overline{V}_{m1}$, as before, but the direction is now almost the same as $\overline{V}_L$. $\overline{V}_{e2}$ as computed by (3) will then be much larger than before and the additional energy will be enough to cause the final orbit to become hyperbolic in an earth-centered coordinate system.

Figure 1c is a superposition of Figure 1a and 1b, with the geometry at $P_1$ shown in detail. Note that point $P_1$ for the slingshot trajectory is somewhat to the left of the same point for the free-return trajectory in an inertial frame. This is understandable since the perturbing velocity impulse was opposite to the velocity vector, and the perturbed orbit therefore lies inside the original one. However, this is more than compensated for by the change in arrival time at the MSI, with the result that $\overline{V}_{m1}$ points to right of the center of the moon, as indicated previously. Thus the time that the vehicle reaches the moving MSI is the important parameter for determining the characteristics of the lunar encounter.

Trajectories which do not lie in the lunar orbital plane are characterized by the dihedral angles $DL_1$, $DL_h$, and $DL_2$, defined as the angles that the lunar orbital plane makes with the trans-lunar, the hyperbolic, and the transearth orbital planes, respectively. For the in-plane case these angles are all zero. Additional information about angle $DL_1$, can be found in Reference 5. As indicated there $DL_1$ can become as large as 62° during the 1969-1970 period. Equations (2) and (3) are still valid when $DL_1 \neq 0$, but the various vector relationships become much more difficult to visualize.

## IV. SLINGSHOT TRAJECTORY CHARACTERISTICS

Free return trajectories were calculated and then

perturbed by changing the velocity vector instantaneously* at a preselected point. A reference set of such trajectories was generated for which the perturbing time is two hours after TLI, and the velocity increment ($\Delta\bar{V}$) is collinear with $\bar{V}$, the velocity vector at the same point. Deviations from these conditions are considered later. The range in $\Delta\bar{V}$ extends from -350 to +100 fps, which is consistent with the amount of fuel remaining in the S-IVB tanks at TLI. (A positive $\Delta V$ is one which is in the same direction as $\bar{V}$.) The periselene distance ($R_{pm}$) of the hyperbola, the energy of the transearth trajectory (ERG), and the perigee of the transearth trajectory ($R_{pe}$) were calculated. A "transparent" moon was assumed, that is, the complete trajectory was calculated even if lunar impact occurred. In this way the various relationships between the variables can be more easily visualized. The results are shown in Figure 2 for $DL_1 = 0$ and 60° with letters A to H on the figure identifying trajectory characteristics. Velocity increment ($\Delta V$) is used as the abscissa in all cases. The lower pair of curves (2c) uses the periselene distance as ordinate and is used for identifying those trajectories which impact the moon. The remaining curves (2a and 2b) refer to the transearth portion of the trajectory which may be either hyperbolic (energy positive), parabolic (energy zero), or elliptic (energy negative). Figure 3 shows the relationship between $DL_1$ and $\Delta V$ for the conditions identified by the letters A to H of Figure 2. As shown there, when $DL_1 = 0$ negative impulses from 1.5 to 60 fps produce lunar impact, 60 to 110 fps produce slingshot, and 110 to 240 fps produce elliptic return orbits. Impulses greater than 240 fps will produce elliptic earth return orbits with perigees less than 5 earth radii. When $DL_1 = 60°$ the above values are reduced by about 25%. The area between A and B of Figure 3 represents trajectories for which $\overline{\Delta V}$ is in the direction of $\bar{V}$, instead of opposite to it.

Two ways of deviating from the reference set of perturbed trajectories were studied. The $\overline{\Delta V}$ vector was placed at an angle to $\bar{V}$ rather than collinear with it, and the perturbing time was delayed to a maximum of 14 hours after TLI. The first method can be subdivided into the in-plane case characterized by the angle $\theta_i$ and the out-of-plane case characterized by the angle $\theta_o$. In the in-plane case $\overline{\Delta V}$ is rotated about $\bar{H}$, a vector perpendicular to the vehicle orbital plane, through the angle $\theta_i$. For the out-of-plane case a vector $\bar{Q}$ is defined which lies in the vehicle orbital plane, perpendicular to $\bar{V}$, and is defined by the equation $\bar{Q} = \bar{V} \times \bar{H}$. $\overline{\Delta V}$ is then rotated about $\bar{Q}$ through the angle $\theta_o$. These quantities

*The dumping process is completed in approximately four minutes. This time is small enough so that it can be considered zero without introducing a significant error.

are illustrated in Figure 4, and the results are shown in Figures 5 through 10. These results will be discussed in the next section.

## V. IMPLEMENTATION OF S-IVB DISPOSAL

In the first method studied the S-IVB is aligned along its negative velocity vector and the propellant dump is terminated when a precalculated $\Delta V$ is attained. The remaining propellant is then vented non-propulsively. The required value of $\Delta V$ is a function of $DL_1$, as shown in curve J of Figure 3, which is drawn in the center of the slingshot region. Note that by this choice the curve is actually biased away from earth impact because of the large $\Delta V$'s required to obtain elliptic orbits of less than 10 earth radii. By positioning this curve the relative probabilities of earth impact and lunar impact, in the presence of guidance errors, can be adjusted.

The minimum $\Delta V$ (143 fps) is established by the trapped residuals and an allowance for expected excess Saturn V performance. If necessary this minimum could be supplemented by the APS. It can be seen that the $\Delta V$ capability will always be sufficient to produce a slingshot in the nominal case. The width of the slingshot corridor for all dihedral angles (area between D and E) is nearly 50 feet/second. Therefore, it should be possible to virtually assure a slingshot trajectory using this method. If TLI errors are larger than approximately 50 feet/second, then ground calculations based on post-TLI tracking would be required to determine the proper propellant dump termination time. The maximum $\Delta V$ available is of no consequence since any excess would be vented non-propulsively.

In the second method studied, the dumping process is not terminated but allowed to continue until all the propellant is exhausted. A coarse control can be obtained by choosing to dump $LH_2$ alone, LOX alone, or both. (The latter would be done sequentially.) Additional control is obtained either by varying the attitude of the S-IVB or by varying the time of the propellant dump. It is necessary to determine an estimate based on the S-IVB second burn duration, of the amount of propellant remaining after TLI.

Figures 5 and 6 show the effect of placing the S-IVB at an angle with $\bar{V}$ for the in-plane case (variations in $\theta_i$) and Figures 7 and 8 give the same information for out-of-plane angles ($\theta_o$). Figures 9 and 10 show the effect of varying the dump time from 2 to 14 hours after TLI. In each figure curve J was drawn through the center of the slingshot region as before.

Figure 6 shows that for $DL_1 = 60°$ (which is the worst case) there is a limitation on the amount of $\Delta V$ that can be accommodated. Positive values of $\theta_i$ result in a wider slingshot corridor than negative values, reaching a maximum width at $\theta_i$ equal to 75°, corresponding to a maximum $\Delta V$ of 190 fps. If a $\Delta V$ greater than 190 fps is to be accommodated path K-K of Figure 6 could be followed, resulting in elongated geocentric elliptic orbits with perigee distances of the order of 20 earth radii. The maximum $\Delta V$ that can be accommodated and result in a perigee greater than 20 earth radii is about 350 fps. These orbits will not intersect the earth for some time; however, as mentioned in Reference (1), the perturbations of the sun and the moon may eventually cause earth impact.

Use of out of plane angles ($\theta_o$) shown in Figures 7 and 8 is restricted to the range from -45° to +45° imposed by the S-IVB navigation system middle gimbal angle limit. It can be seen that with this restriction curve J reaches a maximum $\Delta V$ of 110 fps (using Figure 8). Delaying the time of propellant dump is restricted by S-IVB lifetime. If S-IVB lifetime permits dump maneuvers beyond 2 hours after TLI, Figure 10 indicates that curve J reaches a $\Delta V$ of 150 fps for a delay of 14 hours, and a $\Delta V$ of 100 fps for a delay of 6 hours.

In general, use of an unterminated dump is constrained by the amount of $\Delta V$ that can be accommodated. In the worse case the maximum $\Delta V$ which should not be exceeded to obtain a slingshot trajectory is close to 190 fps with a $\theta_i$ of 75 degrees. In addition, $\Delta V$'s up to 350 fps would result in geocentric elliptical orbits with perigees greater than 20 earth radii.

## VI. RECONTACT

Avoiding recontact between CSM/LM and the S-IVB after withdrawal can be divided into a short-term problem covering a few hours after separation, and a long-term problem, covering the remainder of the mission. In the short-term problem the gravitational field of the earth can be assumed to be the same at the two vehicles. Since both are falling freely, the gravitational field can be ignored when calculating the relative motion. It is apparent then for the short-term case, that the distance between the two vehicles will not decrease as long as an impulse applied to one vehicle does not have a component in the direction of the other vehicle.

The long-term problem involves calculating the position difference of the two vehicles as they move in their respective orbits. Figure 11 illustrates parametrically the long-term recontact problem for a separation $\Delta V$ of -100 fps. It is assumed that the CSM/LM is on a nominal trajectory, with no midcourse correction needed. Note that the portion of the curves near the origin is nearly linear, as predicted above. The upper curve corresponds to a velocity increment which is directed opposite to the velocity vector and is typical of the reference set of trajectories illustrated in Figure 3. The modified orbit lies inside the original orbit and as shown in Figure 11 the separation distance increases uniformly with time. There is therefore no danger of recontact for the reference set of trajectories.

When $\theta_i$ is negative, a component of the velocity increment is in the direction of an inward normal to the orbital curve. The resulting orbit will again lie inside of the original orbit, and no recontact is possible. Positive values of $\theta_i$, however, produce velocity increments which have a component in the direction of the outward normal to the orbital curve. The modified orbit will then lie outside the original orbit for a period of time, after which it crosses the original orbit and enters the interior region. These cases are plotted in Figure 11. Note that in spite of the orbital crossings the separation distance increases uniformly with radial distance, and there is no danger of recontact.

When the velocity increment has a component perpendicular to the vehicle orbital plane (i.e., $\theta_o \neq 0$), a plane change results, and the orbits cannot cross until the true anomaly has increased by 180°. Thus there is no danger of recontact for these cases.

## VII. CONCLUSIONS

Propulsive dumping of the propellant remaining after translunar injection offers a possible method for altering the S-IVB trajectory so that there will be low probability of impacting the earth or moon.

A slingshot trajectory, which is within the propulsive capability of a propellant dump, will safely and effectively dispose of the spent S-IVB. A slingshot can always be obtained by aligning the thrust vector along the vehicle negative velocity vector and applying a measured velocity correction. This method requires the controlled termination of the propellant dump, and has the advantage that large amounts of propellant remaining after TLI can be easily handled.

Another approach is available. The S-IVB could be placed at a precomputed angle to its velocity vector and all

remaining propellant dumped. There is a choice of dumping $LH_2$ alone, LOX alone, or both sequentially. A slingshot trajectory is obtainable for most values of dihedral angle ($DL_1$) when the October 1968 weight and propulsion figures are used. However, excess propellants with increased Saturn V performance may lead to geocentric elliptic orbits which can impact the earth in a few months.

Recontact between the spacecraft and the S-IVB will be avoided in all cases for which the correction has been applied in a direction to increase the probability of a slingshot.

L P Gieseler

2013-LPG-cjz

L. P. Gieseler

Attachments
References
Table I
Figures 1 - 11

TABLE I

ΔV RESULTING FROM PROPELLANT DUMPING

| TYPE | LOX Wt. | LOX ΔV | $LH_2$ Wt. | $LH_2$ ΔV | COMBINED LOX/$LH_2$ Wt. | COMBINED LOX/$LH_2$ ΔV |
|---|---|---|---|---|---|---|
| Excess Performance | 3246 lbs. | 68. fps | 649 lbs. | 27. fps | 3895 lbs. | 95. fps |
| Flight Performance Reserves (FPR) Remaining for High-Performance Vehicle | 3842 | 81. | 768 | 32. | 4610 | 113. |
| Flight Geometry Reserves (FGR) | 1071 | 23. | 214 | 9. | 1285 | 32. |
| Propellant due to Light S/C | 800 | 17. | 200 | 8. | 1000 | 25. |
| Launch Azimuth Variation | 750 | 16. | 150 | 6. | 900 | 22. |
| Trapped Residuals | 473 | 10. | 880 | 38. | 1362 | 48. |
| Total ΔV | | 215. fps | | 120. fps | | 335. fps |

NOTES

1. Either LOX or $LH_2$ may be dumped, or both may be dumped sequentially.
2. The calculation for ΔV was based on the following:
   - Wt. of empty S-IVB + IU = 29000 lbs.
   - $I_{sp}$ of LOX = 19 sec. (Calculated from Reference 6)
   - $I_{sp}$ of $LH_2$ = 38 sec. (Estimated at twice the value for LOX; See Reference 8)
3. The minimum ΔV available is that due to the trapped residuals plus the excess performance or 143 fps
4. The propellant remaining in the APS after TLI is estimated at 123 lbs. Assuming an $I_{sp}$ of 250, this corresponds to a ΔV of 34 fps. However, some of the propellant is required for attitude maneuvers of the S-IVB after TLI.

## REFERENCES


1. "Post Injection Disposal of the S-IVB/IU Stage for a Lunar Mission", MSFC No. R-AERO-DAM-12-67, dated August 30, 1967.

2. Apollo Flight Mission Assignments (U), OMSF Document SE 010-000-1,June 1968, Lunar Landing Mission Appendix P.2.

3. Kraft A. Ehricke, "Space Flight", Vol. II, Dynamics, D. VanNostrand Co., 1962, p. 860-874.

4. "S-IVB Disposal Analysis for the Lunar Landing Mission", by D. C. Daniel, H. L. Hooper, L. V. McWorter, The Boeing Co., No. SSR-166, Dated February 15, 1968.

5. L. P. Gieseler, "The Influence of Earth Launch and Lunar Lighting Constraints on the Apollo Mission", Bellcomm Technical Memorandum TM-67-2013-4, May 26, 1967.

6. "Results of the Fourth Saturn 1B Launch Vehicle Test Flight (AS-204)", MSFC No. MPR-SAT-FE-68-2, dated April 5, 1968.

7. "SSR-228, Saturn V Current Performance, SA-504 through SA-506" Letter No. 5-9600-H-126 from The Boeing Company, Space Division, Launch Systems Branch, to MSFC, dated October 1, 1968.

8. "Performance Analysis of the S-IVB Stage Using Gaseous and Liquid Propellants with or without Combustion", by Klaus W. Gross, MSFC, Propulsion Evaluation Branch, Propulsion Division.

BELLCOMM, INC.

SUBJECT: Disposal of Spent S-IVB Stage on Lunar Missions - Case 310

FROM: L. P. Gieseler

Distribution List

NASA Headquarters

Messrs. T. A. Keegan/MA-2
W. C. Schneider/MA

MSC

Messrs. H. D. Beck/FM5
R. L. Berry/FM5
J. R. Elk/FM5
J. R. Gurley/FM13
C. R. Huss/FM

MSFC

Messrs. R. C. Lester, Jr./R-AERO-DAM
F. E. Swalley/R-P&V-PP
C. L. Thionnet/R-AERO-P
G. Wittenstein/R-AERO-FMT

Abstract Only

Messrs. D. A. Chisholm
D. R. Hagner
B. T. Howard
I. M. Ross
J. W. Timko

Bellcomm, Inc.

Messrs. D. R. Anselmo
A. P. Boysen, Jr.
J. O. Cappellari, Jr.
D. A. Corey
W. G. Heffron
D. B. James
J. L. Marshall, Jr.
J. Z. Menard
V. S. Mummert
P. E. Reynolds
R. V. Sperry
R. L. Wagner
M. T. Yates
Department 1024, Files
Central Files
Library
All Members, Department 2013

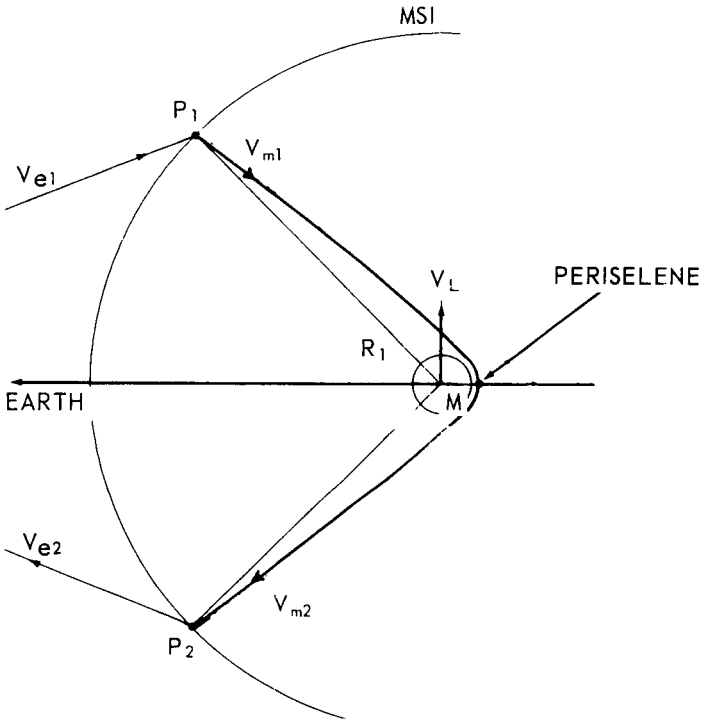


1a – FREE RETURN

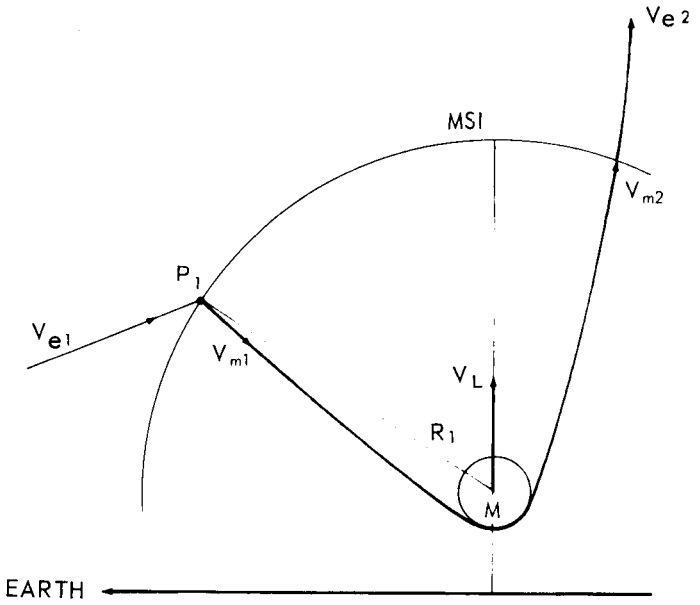


1b – SLINGSHOT

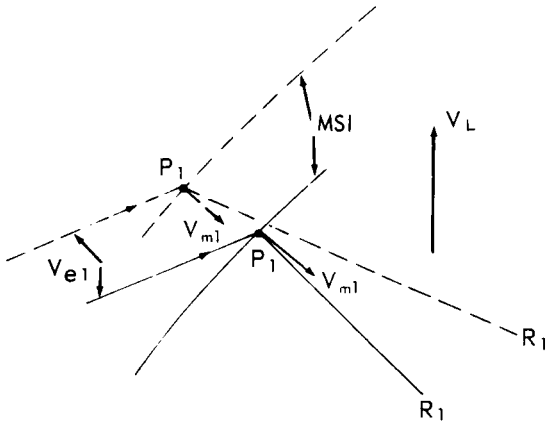


1c – DETAIL AT $P_1$ (DOTTED LINES INDICATE SLINGSHOT CONDITIONS)

$V_{e1}$ – VELOCITY OF VEHICLE IN TRANSLUNAR ELLIPSE
$V_{m1}$, $V_{m2}$ – VELOCITY IN HYPERBOLIC ORBIT AT MSI
$V_{e2}$ – VELOCITY AFTER LEAVING MSI
$R_1$ – SELENOGRAPHIC RADIUS VECTOR
$P_1$, $P_2$ – PIERCING POINTS ON MSI
M – MOON

FIGURE 1 - LUNAR ENCOUNTERS

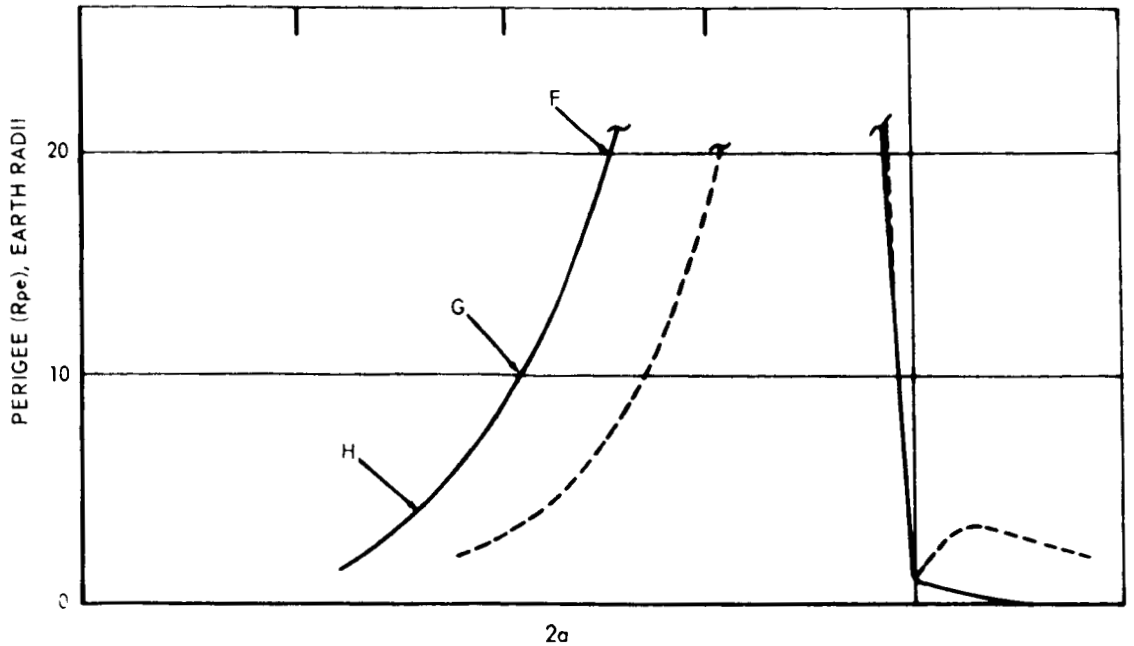


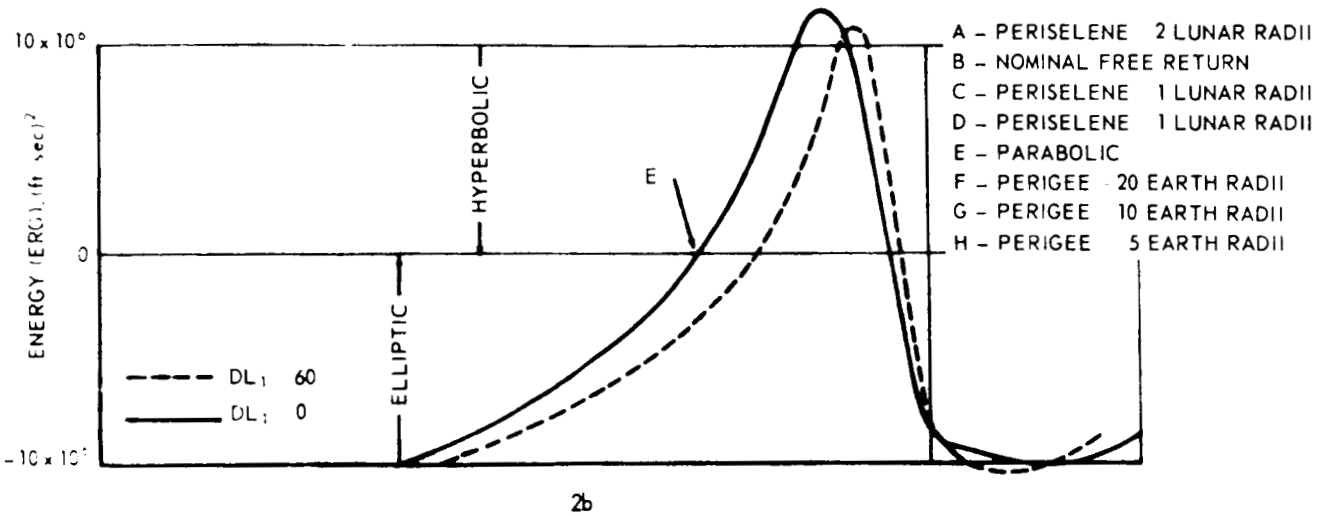


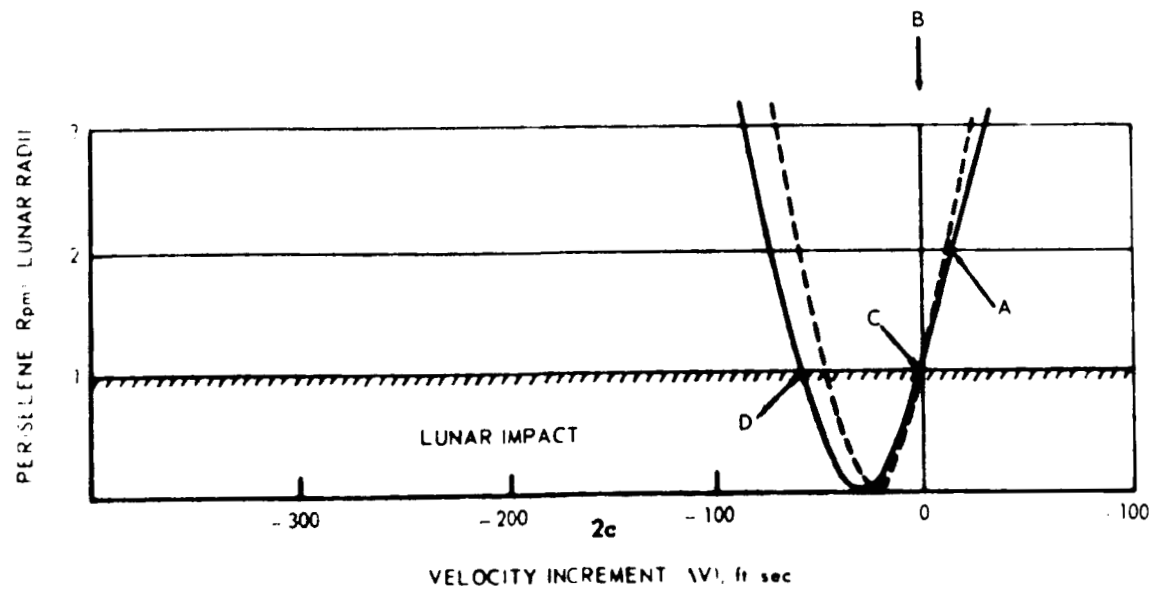


FIGURE 2 - REFERENCE SET OF PERTURBED TRAJECTORIES

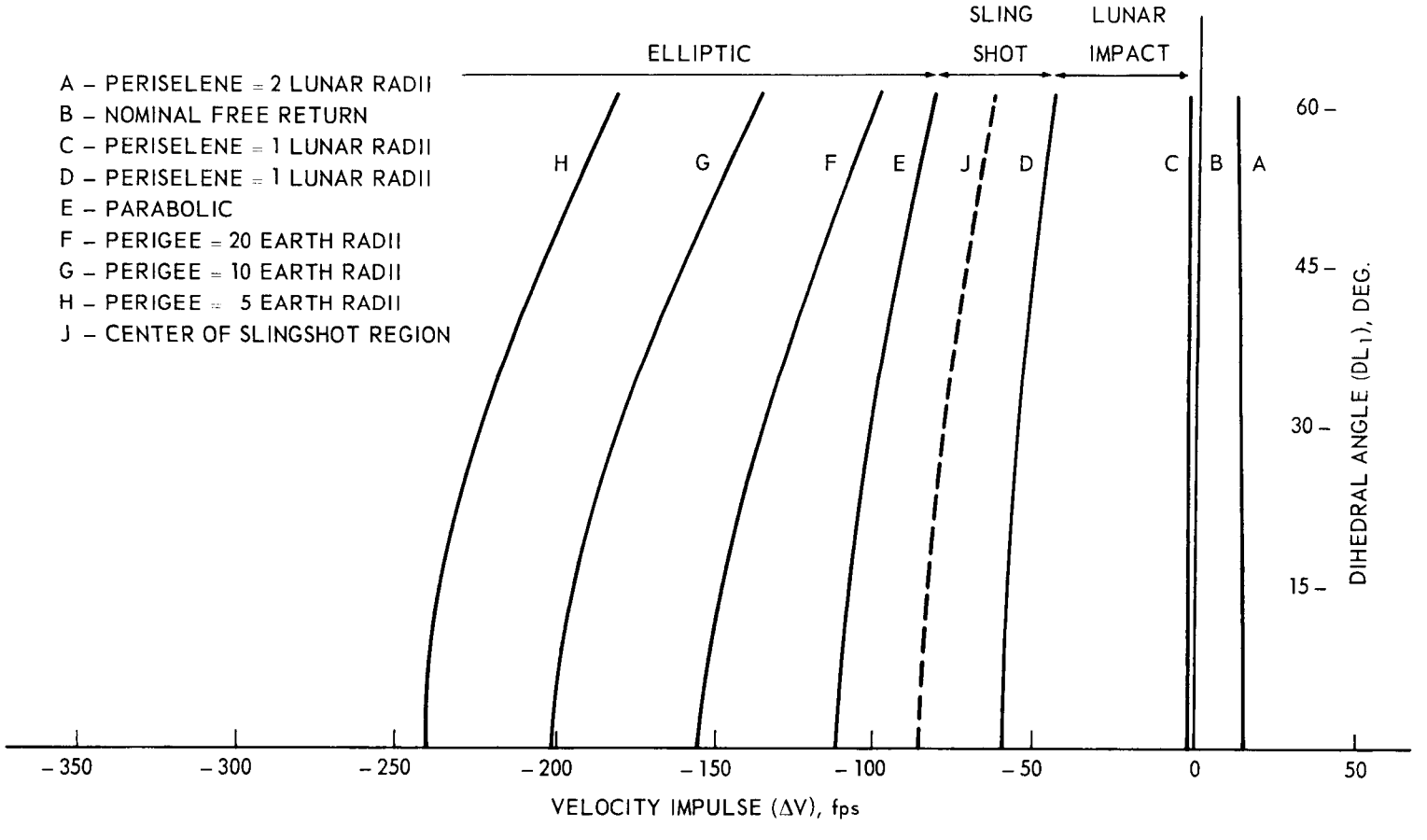


FIGURE 3 - EFFECT OF THE DIHEDRAL ANGLE

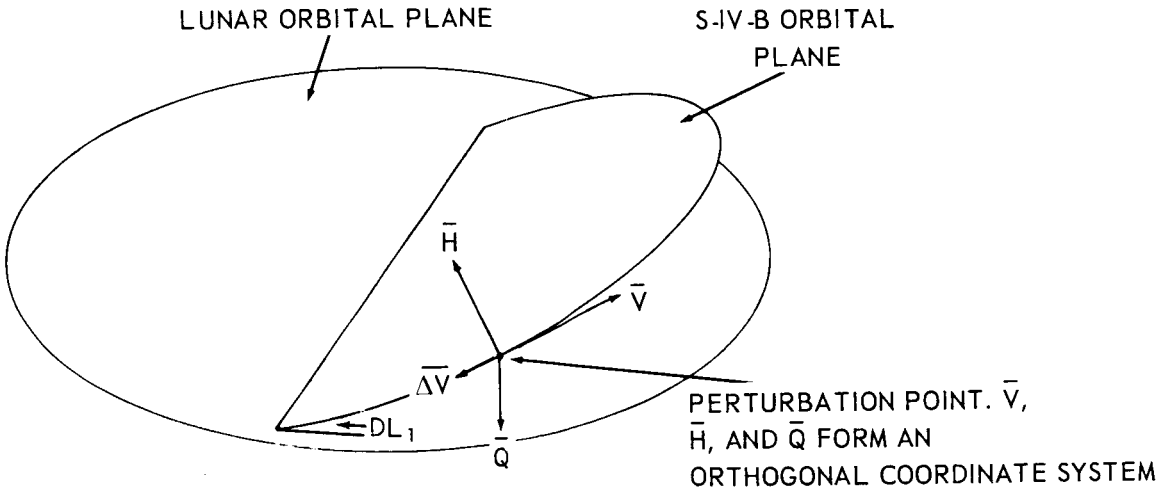


A. ORBITAL PLANES

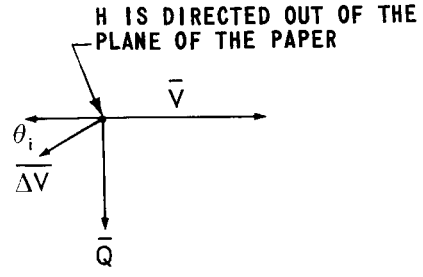


B. IN-PLANE VARIATION OF DIRECTION OF $\Delta\bar{V}$ ($\theta_i$ POSITIVE)

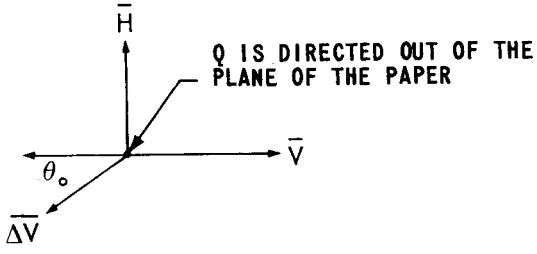


C. OUT-OF-PLANE VARIATION OF DIRECTION OF $\Delta\bar{V}$ ($\theta_o$ POSITIVE)

FIGURE 4 - GEOMETRY OF VELOCITY IMPULSES (A NEGATIVE $\Delta V$ IS ILLUSTRATED)

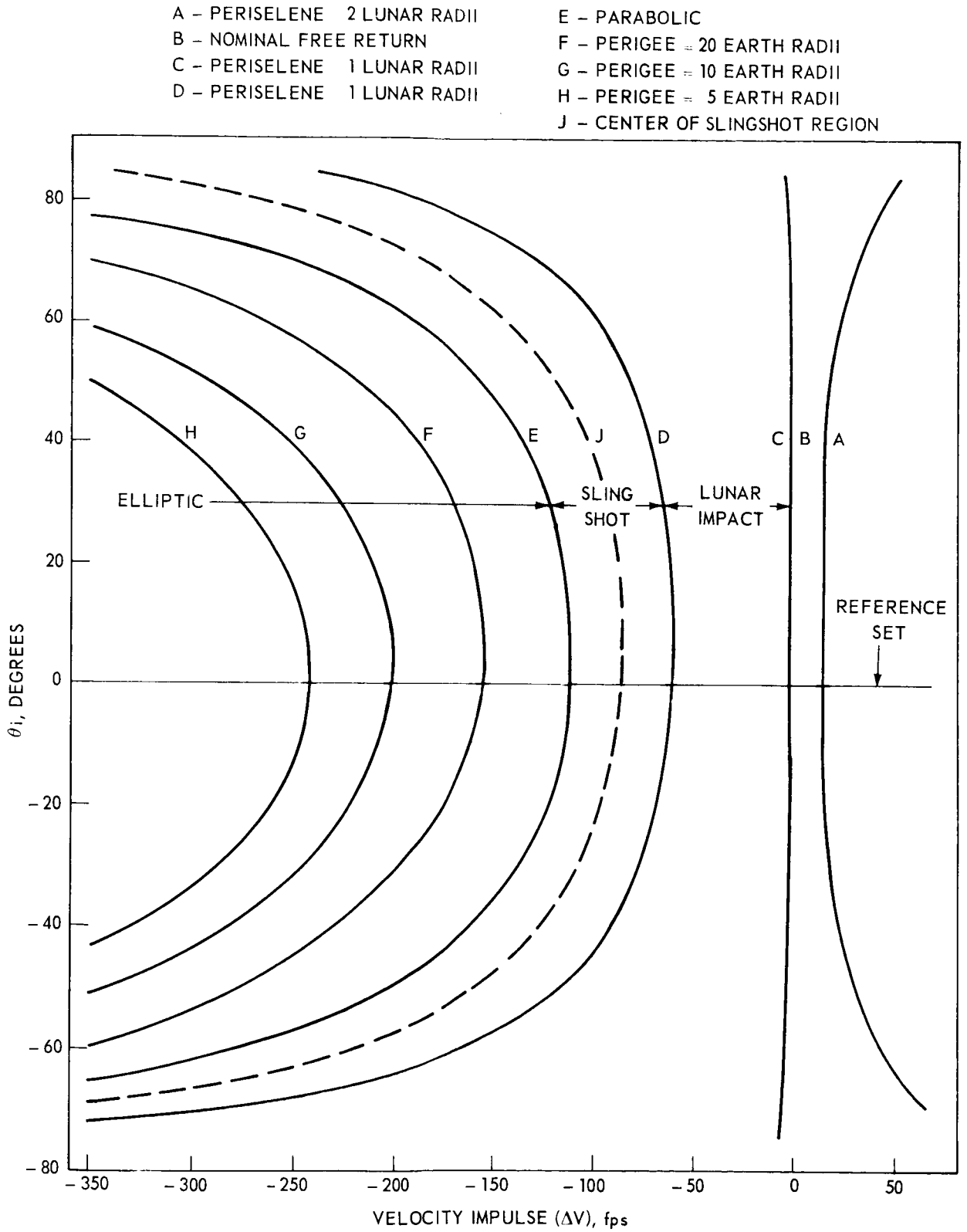


FIGURE 5 - IN-PLANE VARIATION OF DIRECTION OF VELOCITY IMPULSE
($DL_1$=0)

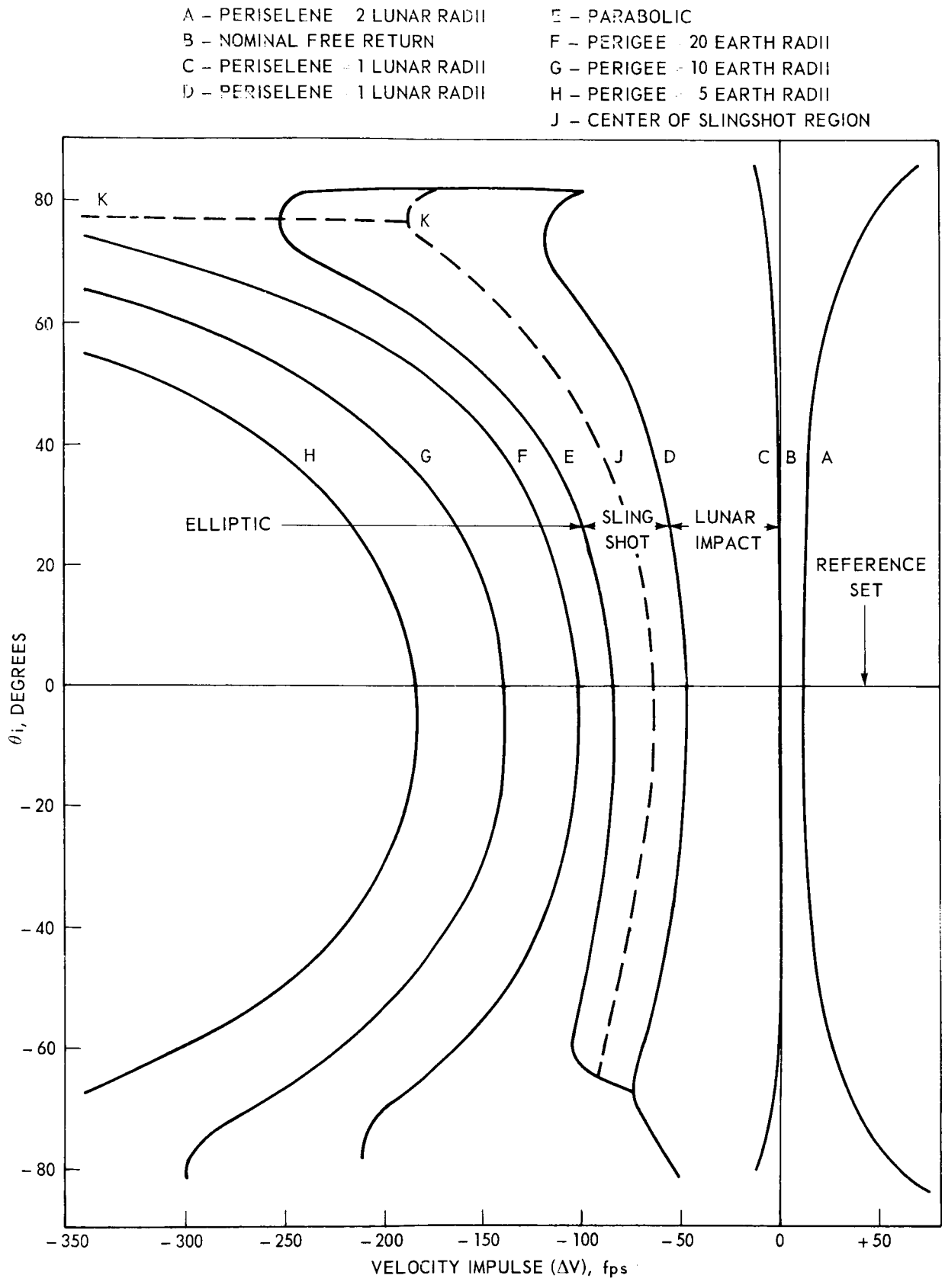


FIGURE 6 - IN-PLANE VARIATION OF DIRECTION OF VELOCITY IMPULSE
($DL_1 = 60^o$)

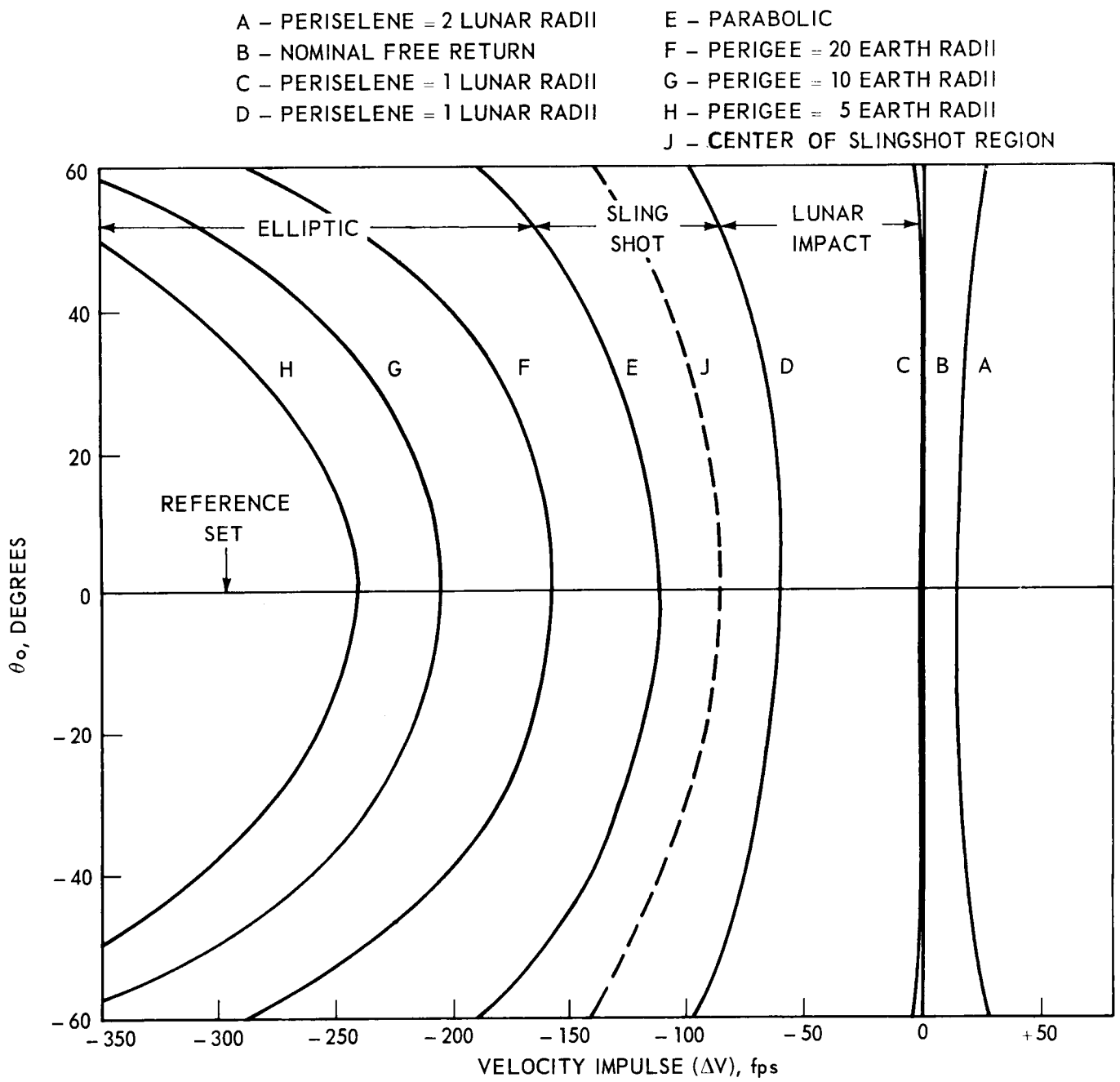


FIGURE 7 - OUT-OF-PLANE VARIATION OF DIRECTION OF VELOCITY IMPULSE ($DL_1$=0)

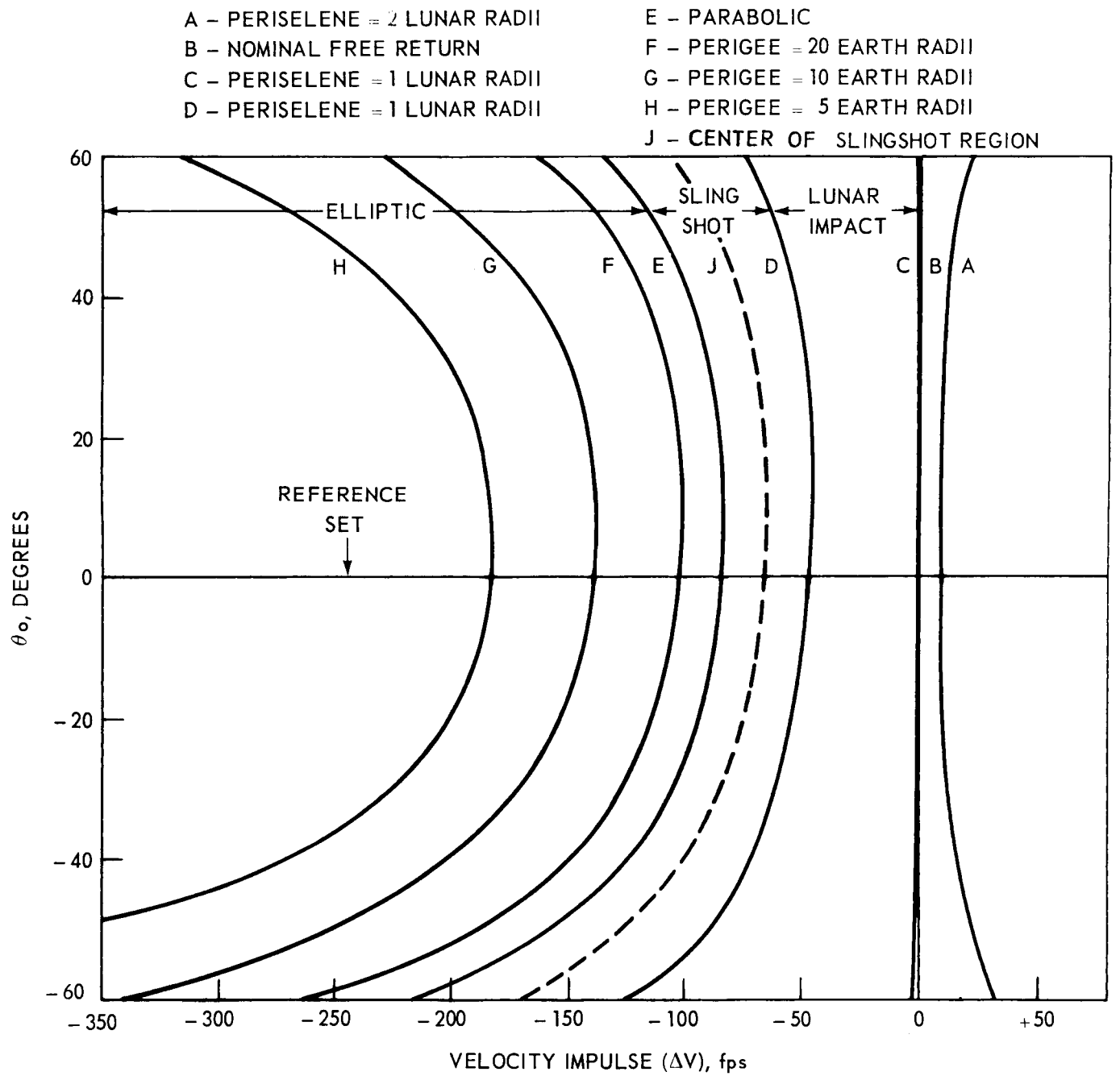


FIGURE 8 - OUT-OF-PLANE VARIATION OF DIRECTION OF VELOCITY IMPULSE ($DL_1=60^o$)

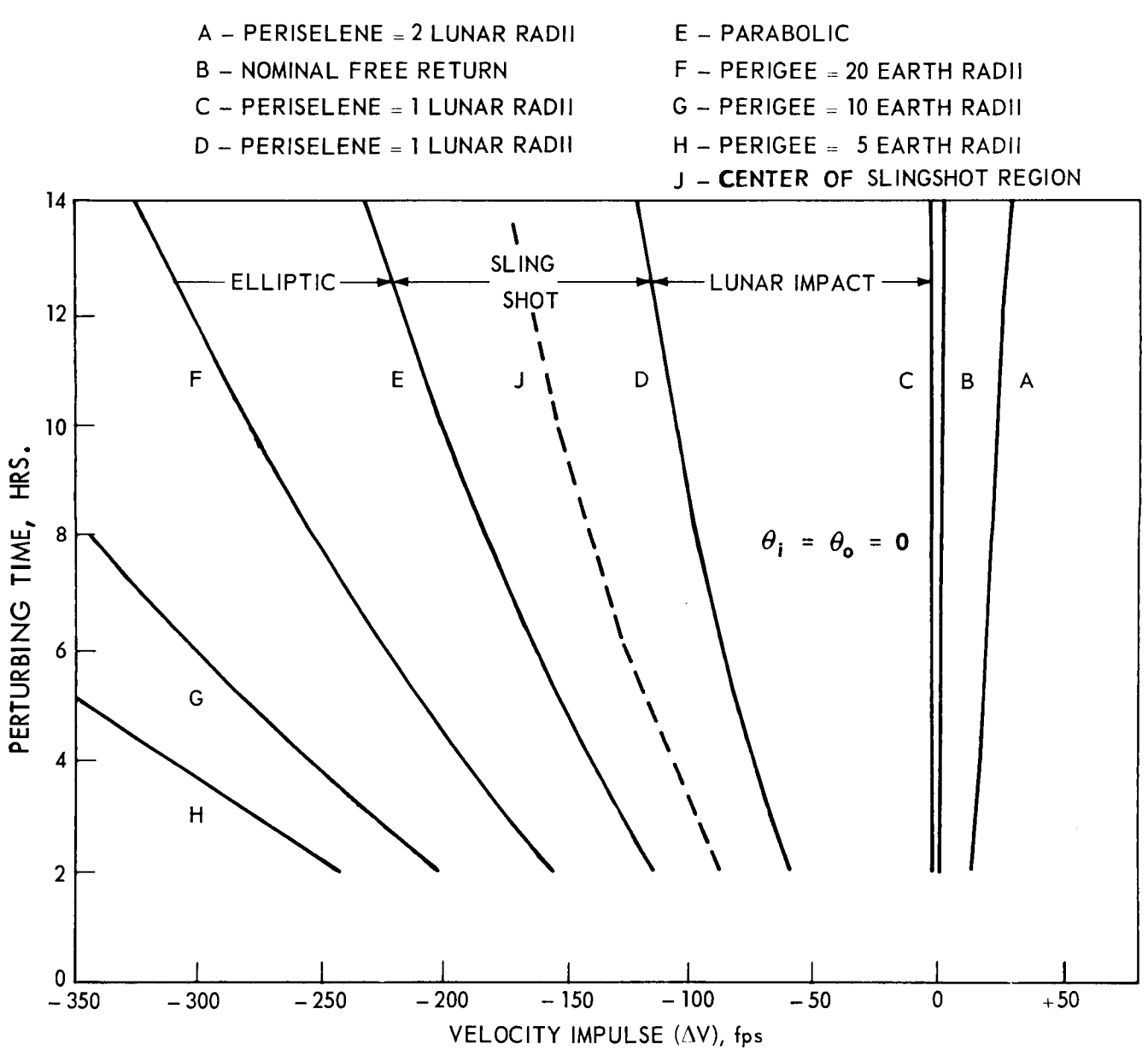


FIGURE 9 - EFFECT OF VARYING PERTURBING TIME
($DL_1$=0)

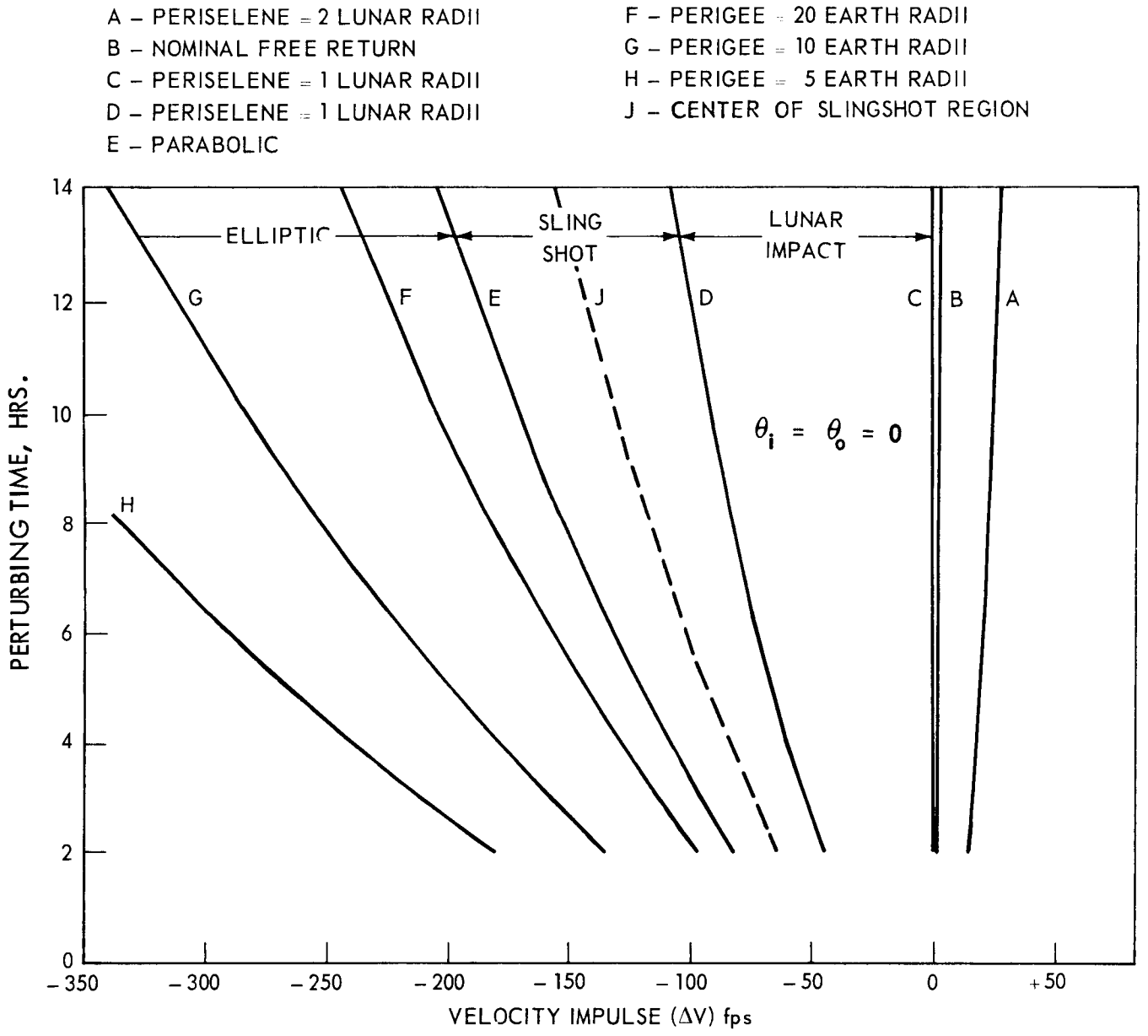


FIGURE 10 - EFFECT OF VARYING PERTURBING TIME
($DL_1$=60°)

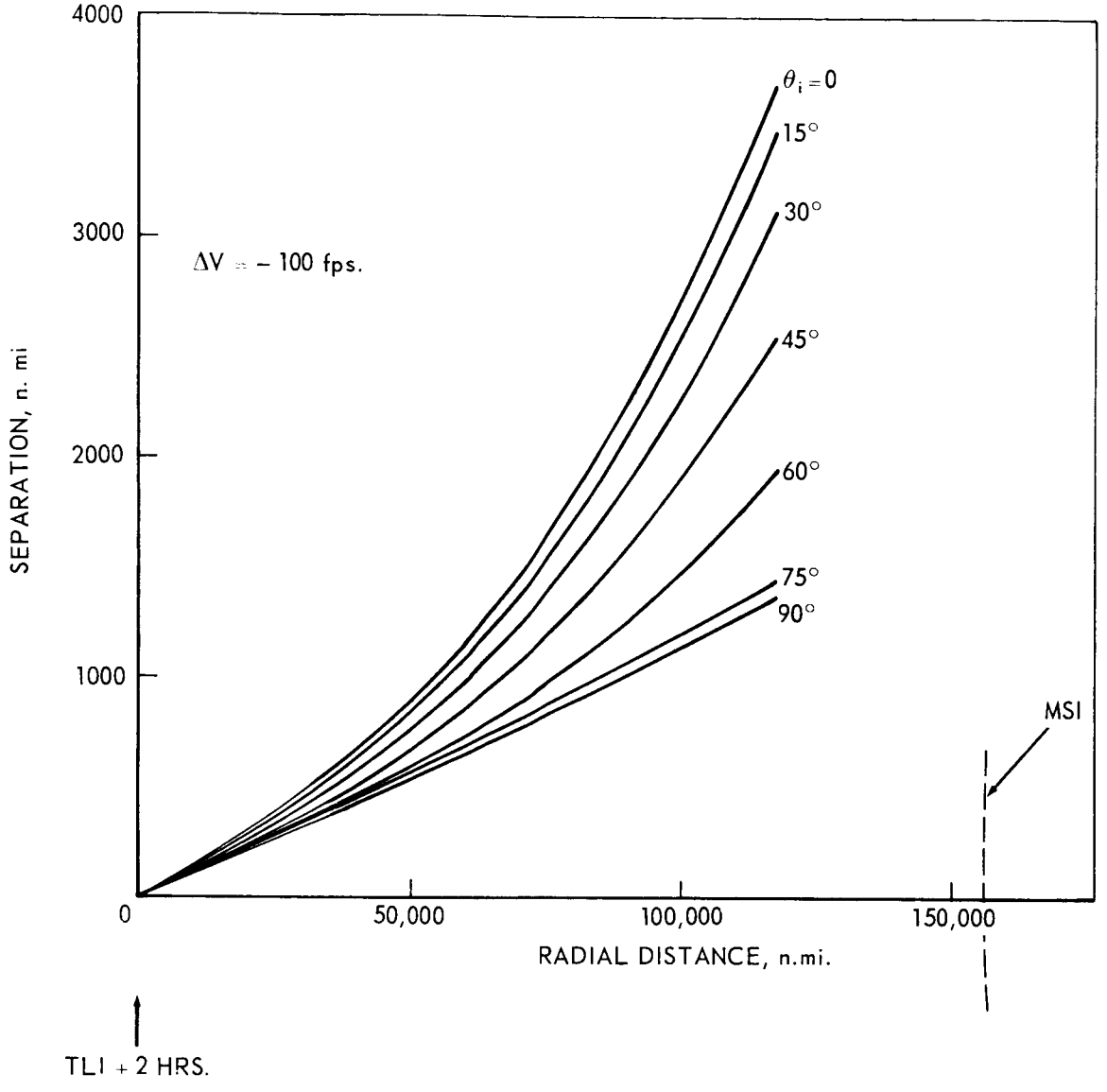


FIGURE 11 - SEPARATION BETWEEN S-IVB AND CSM/LM